J. Fluid Mech. (1993), *vol.* 246, *pp.* 545–568

Mixed mode convection in an inclined slot

By K. FUJIMURA[1] AND R. E. KELLY[2]

[1] Japan Atomic Energy Research Institute, Tokai-mura, Ibaraki 319-11, Japan

[2] Mechanical, Aerospace and Nuclear Engineering Department, University of California, Los Angeles, CA 90024-1597, USA

(Received 15 February 1992 and in revised form 5 August 1992)

Nonlinear interaction between transverse disturbances and longitudinal rolls has been investigated for flow in an inclined slot with a heated lower wall when both modes of instability occur at nearly the same value of the control parameter. This condition is shown to be possible for a fluid with Prandtl number greater than 0.263897. For slightly supercritical values of the Rayleigh number (R) when the critical Rayleigh number for longitudinal rolls R_c^L is somewhat less than that for transverse stationary rolls, R_c^S, and for transverse travelling waves, R_c^T, longitudinal rolls occur first and then remain stable as R is increased beyond R_c^S or R_c^T; no mixed mode state occurs. In contrast, if R_c^S or R_c^T is slightly below R_c^L, pure transverse modes exist for only a relatively small range of R beyond R_c^S or R_c^T. Thereafter, a three-dimensional mixed mode state occurs well before R_c^L is reached, i.e. three-dimensionality sets in on a *subcritical* basis. As R approaches R_c^L, the contribution of the transverse mode decreases continuously until a pure longitudinal roll state emerges for R slightly greater than R_c^L. Mixed mode convection is also investigated for a special choice of parameters when three modes, namely transverse stationary rolls, transverse travelling waves and longitudinal rolls, become unstable simultaneously. Longitudinal rolls again emerge as the stable supercritical state.

1. Introduction

Nonlinear interactions between transverse rolls and longitudinal rolls in Rayleigh–Bénard convection when a mean shear exists have recently attracted increasing attention. For a horizontally unbounded layer, longitudinal rolls with axes in the flow direction are the most unstable mode. Richter (1973) considered a situation for the unbounded case where two-dimensional rolls aligned in one direction are initially excited by means, say, of *thermal imprinting* as first developed by Chen & Whitehead (1968), and so dominate the initial state of convection. A shear flow is then superimposed in the direction perpendicular to the axis of the two-dimensional rolls, which are now called transverse rolls. Deriving coupled amplitude equations and integrating numerically, he demonstrated that after superposition of the shear flow the amplitudes of the transverse rolls decrease while those of longitudinal rolls (given small initial values) increase. After a sufficiently long time, the transverse rolls become negligible, thereby giving rise to a longitudinal roll state. He therefore concluded that the transverse rolls are unstable to longitudinal rolls for any value of the Reynolds number. Richter & Parsons (1975) confirmed experimentally this process of transition between transverse and longitudinal rolls.

With the addition of sidewalls, however, transverse rolls are more unstable at low values of the Reynolds number (Re). Hence there is a cross-over regime of Re

(depending on the aspect ratio) where both modes are important on a nonlinear basis. The idea of a cross-over value of Re, say Re^*, was introduced by Luijkx, Platten & Legros (1981; see also Platten & Legros 1984) for the linear problem. Müller, Lücke & Kamps (1989, 1992) and Brand, Deissler & Ahlers (1991) considered channel flow by using envelope equations. Brand *et al.* considered interaction between transverse and longitudinal rolls. They obtained pure transverse rolls at relatively low values of Re and high values of the Rayleigh number but pure longitudinal rolls for the opposite extreme, in agreement with the linear results. However, Brand *et al.* also obtained a mixed mode composed of these two kinds of roll for some range of parameters. Ouazzani, Platten & Mojtabi (1990) had previously observed a mixed mode state experimentally. Therefore, it would seem that the concept of a unique value of Re^* is an artifice of the linear problem; finite-amplitude states can coexist and give rise to mixed mode convection. It is therefore more accurate to talk about a cross-over regime rather than a cross-over value of Reynolds number.

Another example is an interaction between transverse rolls and near-aligned rolls in a vertical narrow gap between co-rotating concentric cylinders at different uniform temperatures. Kropp & Busse (1991*a*) derived coupled amplitude equations for transverse rolls and near-aligned rolls and obtained typical bifurcation diagrams in which pure transverse rolls, mixed modes, and pure near-aligned rolls exist stably as a sequence of bifurcations.

In the case of pure Rayleigh–Bénard convection in a circular cylinder of finite aspect ratio, different modes become critical depending on the aspect ratio. It should be mentioned that Rosenblat (1982) considered an interaction between different critical modes, derived coupled amplitude equations, and obtained bifurcation diagrams involving a transition from a pure mode to a mixed mode.

In this paper, the case of flow in an inclined slot with a heated lower wall will be discussed. For the case of a vertical slot, transverse stationary rolls exist for $P < 12.454256 \equiv P_c^{ST}$, while a pair of transverse travelling waves exist for $P \geqslant P_c^{ST}$ where P is the Prandtl number; see e.g. Bergholz (1978). Fujimura & Mizushima (1991), Kropp & Busse (1991*b*), and Fujimura (1992) investigated a nonlinear interaction between the stationary mode and the travelling waves on a weakly nonlinear basis for $P \approx P_c^{ST}$. On the other hand, longitudinal rolls exist for a relatively large inclination angle (δ is defined as the angle from the vertical in this paper). A cross-over between transverse and longitudinal disturbances exists as shown by Hart (1971) and Korpela (1974). According to their comparisons, and also to that of Hollands & Konicek (1973), between theoretical predictions and experimental results on this problem, the onset of longitudinal rolls is predicted well by the linear stability theory while the onset of transverse rolls is not predicted so accurately. Hart conjectured that the latter disagreement might be due to the lack of resolution in detecting the onset and also perhaps due to the non-parallelism of the basic flow resulting from end effects of the experimental apparatus with a finite aspect ratio. Unfortunately, these experimental results do not indicate any interaction between longitudinal rolls and transverse ones, although one might expect such interaction just as for the case of Ouazzani *et al.* (1990).

More recently, Kirchartz & Oertel (1988) carried out both a numerical simulation and an experimental observation of this problem in a finite-aspect-ratio box (finite in both width and length). They concluded that within a certain parameter range a stable mixed mode exists although the mode is composed of longitudinal rolls and transverse rolls resulting not from a shear instability but from endwall effects. Shadid & Goldstein (1990) recently reported experimental results for a finite-aspect-

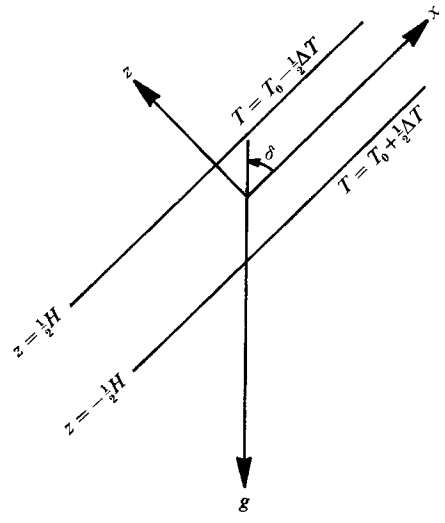

FIGURE 1. Coordinate system of the inclined fluid layer.

ratio box. Although they demonstrated the transition process from transverse to longitudinal rolls with their flow visualization, they did not note the existence of a mixed mode.

The objective of the present paper is to clarify which modes can stably exist in the case of two-mode interaction between transverse disturbances and longitudinal rolls. We classify all the possible equilibrium solutions and also consider their linear stability. We further classify the bifurcation characteristics in the cross-over regime between three modes, i.e. a transverse stationary roll, a pair of transverse travelling waves, and a longitudinal roll, all of which can be critical simultaneously for a suitable choice of parameters.

After describing the mathematical formulation in §2, we discuss the linear stability characteristics in §3, especially in regard to the cross-over feature. We derive the coupled amplitude equations for the interaction between three modes in §4 and obtain equilibrium solutions and their linear stability for two-mode and three-mode cases in §§5 and 6, respectively. In §7, we draw some conclusions.

2. Mathematical formulation

We take the coordinate system (x, y, z) in which two parallel walls are located at $z = \pm\frac{1}{2}H$, and the x-axis is aligned in the direction parallel to the sidewalls. Uniform temperatures on the walls are maintained at $T = T_0 \mp \frac{1}{2}\Delta T$ at $z = \pm\frac{1}{2}H$ as shown in figure 1.

We non-dimensionalize all the quantities by taking the characteristic temperature ΔT, characteristic length H, characteristic velocity, $g\gamma H^2 \Delta T/\nu$, and characteristic time H^2/ν. As a result, we obtain the following system of equations for velocity $\boldsymbol{v}$ and temperature T:

$$\left.\begin{aligned} P^{-1}R[\partial \boldsymbol{v}/\partial t + (\boldsymbol{v}\cdot\boldsymbol{\nabla})\boldsymbol{v}] &= -\boldsymbol{\nabla}p + T\cos\delta\boldsymbol{e}_x + T\sin\delta\boldsymbol{e}_z + \boldsymbol{\nabla}^2\boldsymbol{v}, \\ R[\partial T/\partial t + (\boldsymbol{v}\cdot\boldsymbol{\nabla})T] &= \boldsymbol{\nabla}^2 T, \\ \boldsymbol{\nabla}\cdot\boldsymbol{v} &= 0, \end{aligned}\right\} \tag{2.1}$$

subject to boundary conditions

$$\boldsymbol{v} = 0, \quad T = \mp\tfrac{1}{2} \quad \text{at} \quad z = \pm\tfrac{1}{2}, \tag{2.2}$$

where $R = g\gamma\Delta T H^3/\nu\kappa$ is the Rayleigh number and $P = \nu/\kappa$ is the Prandtl number.

The conduction state ($R < R_c$) has the velocity and temperature profiles

$$\boldsymbol{v} = (\bar{U}(z), 0, 0) = (\tfrac{1}{6}(z^3 - \tfrac{1}{4}z)\cos\delta, 0, 0), \quad T = \bar{T}(z) = -z. \tag{2.3}$$

We introduce a perturbation on the velocity and temperature field as

$$\boldsymbol{v} = \bar{\boldsymbol{v}} + \hat{\boldsymbol{v}} = (\bar{U} + \hat{u}, \hat{v}, \hat{w}), \quad T = \bar{T} + \hat{T}. \tag{2.4}$$

After eliminating the pressure $\hat{p}$, we obtain the final form of the nonlinear disturbance equations, namely

$$\left.\begin{aligned}
&\partial_t(\hat{u}_y - \hat{v}_x) + \bar{U}\partial_x(\hat{u}_y - \hat{v}_x) + \bar{U}'\hat{w}_y \\
&\quad = PR^{-1}[\hat{T}_y\cos\delta + \nabla^2(\hat{u}_y - \hat{v}_x)] - \partial_y(\hat{\boldsymbol{v}}\cdot\nabla)\hat{u} + \partial_x(\hat{\boldsymbol{v}}\cdot\nabla)\hat{v}, \\
&\partial_t\nabla^2\hat{w} + \bar{U}\partial_x\nabla^2\hat{w} - \bar{U}''\hat{w}_x \\
&\quad = PR^{-1}[\nabla_2^2\hat{T}\sin\delta - \hat{T}_{xz}\cos\delta + \nabla^4\hat{w}] \\
&\qquad - \{\nabla^2(\hat{\boldsymbol{v}}\cdot\nabla)\hat{w} - \partial_z[\partial_x(\hat{\boldsymbol{v}}\cdot\nabla)\hat{u} + \partial_y(\hat{\boldsymbol{v}}\cdot\nabla)\hat{v} + \partial_z(\hat{\boldsymbol{v}}\cdot\nabla)\hat{w}]\}, \\
&\partial_t\hat{T} + \bar{U}\hat{T}_x + \bar{T}_z\hat{w} = R^{-1}\nabla^2\hat{T} - (\hat{\boldsymbol{v}}\cdot\nabla)\hat{T}, \\
&\nabla\cdot\hat{\boldsymbol{v}} = 0,
\end{aligned}\right\} \tag{2.5}$$

where a prime denotes differentiation with respect to z and $\nabla_2^2 \equiv \partial^2/\partial x^2 + \partial^2/\partial y^2$. We use the subscripts x, y, z, and t to denote the derivatives of dependent variables.

3. Linear stability characteristics

Let us denote the disturbance as $[\hat{u}, \hat{v}, \hat{w}, \hat{T}]^{\mathrm{T}} \equiv \boldsymbol{\Psi}(x, y, z; t)$. We investigate the linear stability characteristics by the normal mode analysis assuming that

$$\boldsymbol{\Psi} = \boldsymbol{\Phi}(z)\,\mathrm{e}^{\mathrm{i}\alpha(x-ct)+\mathrm{i}\beta y}, \tag{3.1}$$

where $\boldsymbol{\Phi} = [u(z), v(z), w(z), T(z)]^{\mathrm{T}}$, α is the wavenumber of a transverse disturbance, and β is the wavenumber of a longitudinal disturbance.

We only consider a transverse disturbance and a longitudinal disturbance because Gershuni & Zhukhovitskii (1969) demonstrated that oblique modes are never the most unstable. The disturbance equations for longitudinal rolls (L) are

$$S_{(\beta)}^2 w - \beta^2\sin\delta T = 0, \qquad \bar{T}_z w - R^{-1}S_{(\beta)}T = 0, \tag{3.2}$$

while the disturbance equations for transverse stationary rolls (S) or transverse travelling waves (T) are

$$\left.\begin{aligned}
[\mathrm{i}\alpha(\bar{U}-c)S_{(\alpha)} - \mathrm{i}\alpha\bar{U}'' - PR^{-1}S_{(\alpha)}^2]w + PR^{-1}(\alpha^2\sin\delta + \mathrm{i}\alpha D\cos\delta)T = 0, \\
[\mathrm{i}\alpha(\bar{U}-c) - R^{-1}S_{(\alpha)}]T + \bar{T}_z w = 0,
\end{aligned}\right\} \tag{3.3}$$

subject to the homogeneous boundary conditions $w = \mathrm{D}w = T = 0$ at $z = \pm\frac{1}{2}$, where $S_{(\alpha)} \equiv \mathrm{D}^2 - \alpha^2$, $S_{(\beta)} \equiv \mathrm{D}^2 - \beta^2$, and $\mathrm{D} \equiv \mathrm{d}/\mathrm{d}z$.

In order to obtain the critical condition for transverse stationary rolls $(\alpha_c^{\mathrm{S}}, R_c^{\mathrm{S}})$ and that for transverse travelling waves $(\alpha_c^{\mathrm{T}}, R_c^{\mathrm{T}})$, we set $\mathrm{Im}\,c = 0$ and $\partial R/\partial\alpha = 0$ from the start while ignoring the third criticality condition $\partial^2 R/\partial\alpha^2 > 0$. After splitting (3.3) into real and imaginary parts, imposing these two conditions, and expanding (w, T) and $(\partial w/\partial\alpha, \partial T/\partial\alpha)$ as

$$\begin{pmatrix} w \\ \partial w/\partial\alpha \end{pmatrix} = \sum_{n=0}\begin{pmatrix} w^{(n)} \\ w_\alpha^{(n)} \end{pmatrix}(\tfrac{1}{4} - z^2)^2 T_n(2z),$$

$$\begin{pmatrix} T \\ \partial T/\partial\alpha \end{pmatrix} = \sum_{n=0}\begin{pmatrix} T^{(n)} \\ T_\alpha^{(n)} \end{pmatrix}(\tfrac{1}{4} - z^2) T_n(2z),$$

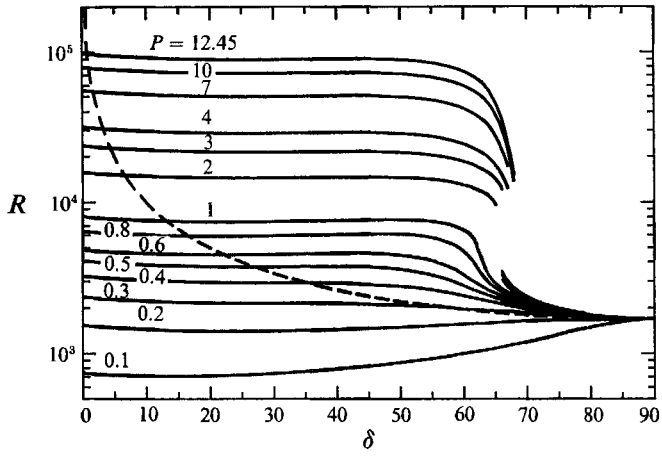

FIGURE 2. Critical Rayleigh number for longitudinal rolls (dashed line) and for transverse stationary rolls (solid lines). A cross-over point is where two modes share the same critical Rayleigh number.

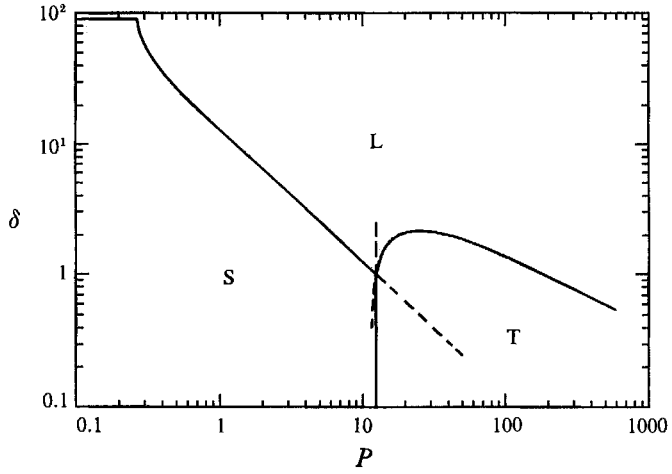

FIGURE 3. Cross-over points among different modes (solid lines). Label S denotes the region in which a transverse stationary roll gives the critical condition, T denotes the one in which transverse travelling waves give the critical condition, and L denotes the one in which a longitudinal roll gives the critical condition. Dashed lines denote extensions of solid lines.

we reduce the linear system (3.3) subject to homogeneous boundary conditions to simultaneous nonlinear algebraic equations for $[w^{(n)}, w_\alpha^{(n)}]^{\mathrm{T}}$, $[T^{(n)}, T_\alpha^{(n)}]^{\mathrm{T}}$, c_{r}, $\partial c_{\mathrm{r}}/\partial\alpha$, α_{c}, and R_{c}. Here $T_n(2z)$ denotes the Chebyshev polynomial of the nth degree and the factors $(\frac{1}{4}-z^2)^2$ and $(\frac{1}{4}-z^2)$ are involved in the expansion functions in order that the functions satisfy the boundary conditions automatically. To solve the equations, we utilized the Newton method. The critical condition for longitudinal rolls is independent of the Prandtl number and is simply given as

$$\beta = 3.1163236, \quad R_{\mathrm{c}}^{\mathrm{L}} = 1707.7618/\sin\delta.$$

We depict $R_{\mathrm{c}}^{\mathrm{S}}$ as a function of the inclination angle δ for several values of P in figure 2. At the intersection between the curves for the longitudinal rolls, $R_{\mathrm{c}}^{\mathrm{L}}$, and the curves for the transverse rolls, $R_{\mathrm{c}}^{\mathrm{S}}$, the longitudinal roll and transverse roll share the critical

	P	δ	R
S–L	12.420013	1.0065474	97216.060
	10	1.2523682	78136.236
	7	1.7954436	54506.618
	1	13.109803	7529.2181
	0.7	18.824115	5292.6923
T–L	12.420013	1.0065474	97216.060
	50	1.8497816	52905.997
	100	1.3639647	71744.366
	200	0.9592889	102004.84
	500	0.5873833	166585.02
S–T	12.420013	1.0065474	97216.060
	12.431822	0.7	97466.817
	12.441431	0.4	97715.228
	12.447841	0.2	97882.506
	12.454256	0.0	98051.132

TABLE 1. Cross-over points for typical Prandtl numbers.

condition. For $P \geqslant 2$, the curves for R_c^S show discontinuity and many-valuedness for $65° \leqslant \delta \leqslant 70°$, corresponding to the *closed disconnected neutral curves* discussed by Chen & Pearlstein (1989).

We summarize the distribution of the cross-over points between L and S, between L and T, and between T and S in the (P, δ)-plane in figure 3. We find that the S mode always dominates for $P \leqslant 0.263897$ if $\delta < 90°$. The same diagram has been obtained by Korpela (1974). For $P \gg 1$, our diagram for L–S has the asymptotic behaviour $\delta \sim 12.533 P^{-1.0019}$ while Korpela's result does not have such a clear asymptote for $P \gg 1$. The diagram for L–T shows $\delta \sim 17.156 P^{-0.54299}$ for $P \gg 1$. The curve for T–S is almost vertical but slightly inclined with very large negative slope. The Prandtl number on this curve tends to $P = 12.454256$ as $\delta \to 0$. These three curves intersect at $(P_c, \delta_c, R_c) = (12.420013, 1.0065474, 97216.060)$ which is the condition for three-mode interaction. We tabulate some typical data on these curves in table 1.

4. Weakly nonlinear reduction of amplitude equations

We describe only the essentials of how to derive the coupled amplitude equations on a weakly nonlinear basis in the neighbourhood of the point at which three modes, (S), (T), and (L), simultaneously bifurcate. The derivation for the two-mode interaction is included in the following as a subset. We expand $\boldsymbol{\Psi}$ about the crossover point (P_c, δ_c, R_c) in $P_c R_c^{-1} - P R^{-1} \equiv \epsilon^2, P_c^{-1} - P^{-1} \equiv \epsilon^2 \tilde{P}$, and $\delta - \delta_c \equiv \epsilon^2 \tilde{\delta}$ as

$$\boldsymbol{\Psi} = (\epsilon \boldsymbol{\Psi}_1 + \epsilon^3 \boldsymbol{\Psi}_1^{(1)} + \ldots) E_1 + (\epsilon \boldsymbol{\Psi}_2 + \epsilon^3 \boldsymbol{\Psi}_2^{(1)} + \ldots) E_2 + (\epsilon \boldsymbol{\Psi}_3 + \epsilon^3 \boldsymbol{\Psi}_3^{(1)} + \ldots) E_3$$

$$+ (\epsilon \boldsymbol{\Psi}_4 + \epsilon^3 \boldsymbol{\Psi}_4^{(1)} + \ldots) E_4 + \epsilon^2 \sum_{m,n=-4} \boldsymbol{\Psi}_{mn} E_m E_n + \text{h.o.t.} + \text{c.c.}, \quad (4.1)$$

where $E_n \equiv \mathrm{e}^{\mathrm{i}\alpha_n(x - c_n t) + \mathrm{i}\beta_n y}$ and $E_{-n} = E_n^{-1}$. We label the pair of transverse travelling waves as $n = 1$, 2, transverse stationary rolls as $n = 3$, and longitudinal rolls as $n = 4$ so that $\alpha_1 = \alpha_2, \beta_1 = \beta_2 = 0$, $\beta_3 = 0$, and $\alpha_4 = 0$. Moreover, $c_3 = c_4 = 0$, and $c_1 = -c_2$. For simplicity, let

$$\alpha_m + \alpha_n + \ldots \equiv \alpha_{mn\ldots}, \quad \beta_m + \beta_n + \ldots \equiv \beta_{mn\ldots}, \quad \text{and} \quad \alpha_m c_m + \alpha_n c_n + \ldots \equiv (\alpha c)_{mn\ldots}.$$

For later convenience, we introduce the following linear operators

$$\mathrm{L}_{mn} \equiv \begin{pmatrix} \beta_{mn}\mathscr{M}_{mn} & -\alpha_{mn}\mathscr{M}_{mn} & \mathrm{i}\beta_{mn}\bar{U}' & -\mathrm{i}\beta_{mn}P_{\mathrm{c}}R_{\mathrm{c}}^{-1}\cos\delta_{\mathrm{c}} \\ \mathrm{i}\alpha_{mn} & \mathrm{i}\beta_{mn} & \mathrm{D} & 0 \\ 0 & 0 & \mathscr{L}_{mn} & P_{\mathrm{c}}R_{\mathrm{c}}^{-1}(\gamma_{mn}^2\sin\delta_{\mathrm{c}}+\mathrm{i}\alpha_{mn}\mathrm{D}\cos\delta_{\mathrm{c}}) \\ 0 & 0 & \bar{T}_z & -\mathrm{i}(\alpha c)_{mn}+\mathrm{i}\alpha_{mn}\bar{U}-R_{\mathrm{c}}^{-1}S_{mn} \end{pmatrix},$$

$$\mathrm{L}_{mn,\delta} \equiv \begin{pmatrix} -\alpha_{mn}\beta_{mn}\dot{\bar{U}} & \alpha_{mn}^2\dot{\bar{U}} & \mathrm{i}\beta_{mn}\dot{\bar{U}}' & \mathrm{i}\beta_{mn}P_{\mathrm{c}}R_{\mathrm{c}}^{-1}\sin\delta_{\mathrm{c}} \\ 0 & 0 & 0 & 0 \\ 0 & 0 & \mathrm{i}\alpha_{mn}\dot{\bar{U}}\mathrm{S}_{mn}-\mathrm{i}\alpha_{mn}\dot{\bar{U}}'' & P_{\mathrm{c}}R_{\mathrm{c}}^{-1}(\gamma_{mn}^2\cos\delta_{\mathrm{c}}-\mathrm{i}\alpha_{mn}\mathrm{D}\sin\delta_{\mathrm{c}}) \\ 0 & 0 & 0 & \mathrm{i}\alpha_{mn}\dot{\bar{U}} \end{pmatrix},$$

$$\mathrm{L}_{mn,P^{-1}R} \equiv \begin{pmatrix} -\mathrm{i}\beta_{mn}\mathrm{S}_{mn} & \mathrm{i}\alpha_{mn}\mathrm{S}_{mn} & 0 & -\mathrm{i}\beta_{mn}\cos\delta_{\mathrm{c}} \\ 0 & 0 & 0 & 0 \\ 0 & 0 & -\mathrm{S}_{mn}^2 & \gamma_{mn}^2\sin\delta_{\mathrm{c}}+\mathrm{i}\alpha_{mn}\mathrm{D}\cos\delta_{\mathrm{c}} \\ 0 & 0 & 0 & -P_{\mathrm{c}}^{-1}\mathrm{S}_{mn} \end{pmatrix},$$

$$\mathrm{L}_{mn,P} \equiv \begin{pmatrix} 0 & 0 & 0 & 0 \\ 0 & 0 & 0 & 0 \\ 0 & 0 & 0 & 0 \\ 0 & 0 & 0 & -P_{\mathrm{c}}R_{\mathrm{c}}^{-1}\mathrm{S}_{mn} \end{pmatrix}, \quad \mathrm{M}_{mn} \equiv \begin{pmatrix} \mathrm{i}\beta_{mn} & -\mathrm{i}\alpha_{mn} & 0 & 0 \\ 0 & 0 & 0 & 0 \\ 0 & 0 & \mathrm{S}_{mn} & 0 \\ 0 & 0 & 0 & 1 \end{pmatrix},$$

where

$$\mathscr{L}_{mn} = \mathrm{i}[\alpha_{mn}\bar{U}-(\alpha c)_{mn}]\mathrm{S}_{mn}-\mathrm{i}\alpha_{mn}\bar{U}''-P_{\mathrm{c}}R_{\mathrm{c}}^{-1}\mathrm{S}_{mn}^2,$$
$$\mathscr{M}_{mn} = (\alpha c)_{mn}-\alpha_{mn}\bar{U}-\mathrm{i}P_{\mathrm{c}}R_{\mathrm{c}}^{-1}\mathrm{S}_{mn},$$
$$\gamma_{mn}^2 = \alpha_{mn}^2+\beta_{mn}^2, \quad \dot{\bar{U}} \equiv \partial\bar{U}/\partial\delta, \quad \mathrm{S}_{mn} \equiv \mathrm{D}^2-\gamma_{mn}^2.$$

We make use of the method of multiple scales so that we set

$$t_n = \epsilon^{2n}t, \quad n = 0,1,2,\ldots, \quad \frac{\partial}{\partial t} = \sum_{j=0}\epsilon^{2j}\frac{\partial}{\partial t_j}. \tag{4.2}$$

In particular, $t_1 = \epsilon^2 t$. At $O(\epsilon)$ we obtain the linear equations

$$L_j\boldsymbol{\Psi}_j = 0, \quad j = 1,2,3,4, \tag{4.3}$$

which are consistent with either (3.2) or (3.3). The solution $\boldsymbol{\Psi}_j$ is obtained in the form of

$$\boldsymbol{\Psi}_j = A_j(t_1,\ldots)\boldsymbol{\Phi}_j(z). \tag{4.4}$$

The eigenfunction $\boldsymbol{\Phi}_j(z)$ is normalized such that $w_j(0) = 1$.

Derivation of the equations at $O(\epsilon^2)$ is straightforward. We note here that the mean flow distortion $\boldsymbol{\Psi}_0$ must satisfy the constant mass flux condition in order to be relevant to flow within a slot with endwalls.

At $O(\epsilon^3)$, we obtain four inhomogeneous equations of the form of

$$L_j\boldsymbol{\Psi}_j^{(1)} = -M_j\boldsymbol{\Phi}_j\frac{\partial A_j}{\partial t_1}+A_j\sum_{k=1}^{4}|A_k|^2\boldsymbol{N}_{-kkj}+\sigma_j\boldsymbol{\Phi}_jA_j, \tag{4.5}$$

where $\sigma_j \equiv L_{j,P^{-1}R}-\tilde{\delta}L_{j,\delta}+\tilde{P}L_{j,P}$ and $\boldsymbol{N}_{-kkj}$ denote the nonlinear term whose explicit form is not listed here. The solvability condition for $\boldsymbol{\Psi}_j^{(1)}$ yields coupled amplitude equations of the form of

$$\frac{\mathrm{d}A_j}{\mathrm{d}t_1} = \tilde{\lambda}_jA_j+\sum_{k=1}^{4}\lambda_{-kkj}|A_k|^2A_j, \quad j = 1,2,3,4, \tag{4.6}$$

$\lambda_3^{(G)}$	4.2419274×10^{1}	$\lambda_4^{(G)}$	2.6158226
$\lambda_3^{(P)}$	-5.0019071×10^{-5}	$\lambda_4^{(P)}$	2.3515549×10^{-3}
$\lambda_3^{(\delta)}$	1.7417820×10^{-3}	$\lambda_4^{(\delta)}$	1.0716816×10^{-2}
λ_{-333}	-8.3859831×10^{4}	λ_{-334}	3.0332176×10^{4}
λ_{-443}	-2.3307004×10^{7}	λ_{-444}	-2.8534022×10^{4}

TABLE 2. Coefficients involved in coupled amplitude equations for the S–L interaction evaluated at $(P,R,\delta)=(7,\ 54506.618,\ 1.7954436)$.

	Real part	Imaginary part
$\lambda_1^{(G)}=\lambda_2^{(G)*}$	7.4993746×10^{-1}	3.2439113×10^{-1}
$\lambda_1^{(P)}=\lambda_2^{(P)*}$	5.5942236×10^{-2}	-3.2290664×10^{-2}
$\lambda_1^{(\delta)}=\lambda_2^{(\delta)*}$	1.9297902×10^{-3}	1.8432297×10^{-3}
$\lambda_{-111}=\lambda_{-222}^{*}$	-8.2701212×10^{3}	9.7993298×10^{3}
$\lambda_{-221}=\lambda_{-112}^{*}$	9.7692758×10^{2}	-5.0040034×10^{3}
$\lambda_{-331}=\lambda_{-332}^{*}$	-1.0571395×10^{8}	-9.2328355×10^{7}
$\lambda_3^{(G)}$	1.9549109×10^{-1}	0
$\lambda_3^{(P)}$	2.7248285×10^{-2}	0
$\lambda_3^{(\delta)}$	1.1443968×10^{-2}	0
$\lambda_{-113}=\lambda_{-223}^{*}$	5.0048593×10^{4}	6.6524787×10^{-5}
λ_{-333}	-4.0124209×10^{4}	0

TABLE 3. Coefficients involved in coupled amplitude equations for the T–L interaction evaluated at $(P,R,\delta)=(100,\ 71744.366,\ 1.3639647)$.

where

$$\tilde{\lambda}_j\equiv\langle\sigma_j\boldsymbol{\Phi}_j\rangle_j=\langle L_{j,P^{-1}R}\boldsymbol{\Phi}_j\rangle_j+\tilde{\delta}\langle -L_{j,\delta}\boldsymbol{\Phi}_j\rangle_j+\tilde{P}\langle L_{j,P}\boldsymbol{\Phi}_j\rangle_j$$
$$\equiv\lambda_j^{(G)}+\tilde{\delta}\lambda_j^{(\delta)}+\tilde{P}\lambda_j^{(P)}.$$

Also,
$$\lambda_{-kkj}\equiv\langle N_{-kkj}\rangle_j,$$

where
$$\langle f(z)\rangle_j\equiv\int_{-\frac{1}{2}}^{\frac{1}{2}}f(z)\,\tilde{\boldsymbol{\Phi}}_j\,\mathrm{d}z\Big/\int_{-\frac{1}{2}}^{\frac{1}{2}}\tilde{\boldsymbol{\Phi}}_j M_j\boldsymbol{\Phi}_j\,\mathrm{d}z,$$

and $\tilde{\boldsymbol{\Phi}}_j(z)=[0,0,\tilde{w},\tilde{T}]^{\mathrm{T}}$ is the adjoint function of $\boldsymbol{\Phi}_j(z)$ defined by

$$-P_{\mathrm{c}}R_{\mathrm{c}}^{-1}S_j^2\tilde{w}+\bar{T}_z\tilde{T}=0,\quad P_{\mathrm{c}}\beta_j^2\tilde{\omega}\sin\delta_{\mathrm{c}}-S_j\tilde{T}=0 \tag{4.7}$$

for the longitudinal roll, while

$$\left.\begin{aligned}&[\mathrm{i}\alpha_j\bar{U}S_j-\mathrm{i}(\alpha c)_jS_j+2\mathrm{i}\alpha_j\bar{U}'\mathrm{D}-P_{\mathrm{c}}R_{\mathrm{c}}^{-1}S_j^2]\tilde{w}+\bar{T}_z\tilde{T}=0,\\&P_{\mathrm{c}}R_{\mathrm{c}}^{-1}(\alpha_j^2\sin\delta_{\mathrm{c}}-\mathrm{i}\alpha_j\cos\delta_{\mathrm{c}}\,\mathrm{D})\tilde{w}+[-\mathrm{i}(\alpha c)_j+\mathrm{i}\alpha_j\bar{U}-R^{-1}S]\tilde{T}=0\end{aligned}\right\} \tag{4.8}$$

for the transverse disturbances, both equations being subject to homogeneous boundary conditions.

Coefficients involved in (4.6) are evaluated numerically at $P=7$, 100, and 12.420013 and are tabulated in tables 2, 3, and 4, respectively.

5. Bifurcation for two-mode interaction

In the following sections concerning analysis of the amplitude equations, for simplicity we utilize the original timescale t instead of the slow ones, $t_n, n\geqslant 1$. Let us start with the interaction between transverse stationary rolls and longitudinal

	Real part	Imaginary part
$\lambda_1^{(G)} = \lambda_2^{(G)*}$	3.0878922×10^{-1}	2.8270393
$\lambda_1^{(P)} = \lambda_2^{(P)*}$	3.5754725×10^{-3}	$-2.2486003 \times 10^{-3}$
$\lambda_1^{(\delta)} = \lambda_2^{(\delta)*}$	5.5561793×10^{-5}	2.4748060×10^{-4}
$\lambda_{-111} = \lambda_{-222}^*$	-3.9807707×10^{4}	2.9002831×10^{4}
$\lambda_{-221} = \lambda_{-112}^*$	4.4817678×10^{3}	-2.4937499×10^{3}
$\lambda_{-331} = \lambda_{-332}^*$	8.6821267×10^{3}	2.0243108×10^{4}
$\lambda_{-441} = \lambda_{-442}^*$	-6.8324086×10^{7}	-1.6135646×10^{7}
$\lambda_3^{(G)}$	4.2599543×10^{1}	0.0
$\lambda_3^{(P)}$	$-5.1748696 \times 10^{-5}$	0.0
$\lambda_3^{(\delta)}$	1.8041695×10^{-3}	0.0
$\lambda_{-113} = \lambda_{-223}^*$	6.6742016×10^{4}	7.5087195×10^{4}
λ_{-333}	-1.7504458×10^{5}	0.0
λ_{-443}	-7.0672793×10^{7}	0.0
$\lambda_4^{(G)}$	1.5194595	0.0
$\lambda_4^{(P)}$	2.4109890×10^{-3}	0.0
$\lambda_4^{(\delta)}$	1.1048845×10^{-2}	0.0
$\lambda_{-114} = \lambda_{-224}^*$	3.1731141×10^{5}	1.1368121×10^{1}
λ_{-334}	3.2400366×10^{4}	0.0
λ_{-444}	-5.2464715×10^{4}	0.0

TABLE 4. Coefficients involved in coupled amplitude equations for interaction among the S, T, and L modes evaluated at $(P, R, \delta) = (12.420013, 97216.060, 1.0065474)$.

rolls in the neighbourhood of the cross-over region. If we set $\epsilon A_j = a_j(t)\,\mathrm{e}^{\mathrm{i}\theta(t)}$ and $\epsilon^2 \tilde{\lambda}_j = \lambda_j$, the amplitude equations for A_3 and A_4 are written in the form

$$\frac{\mathrm{d}a_3}{\mathrm{d}t} = a_3\left(\lambda_3 + \sum_{j=3}^{4} \lambda_{-jj3} a_j^2\right), \quad \frac{\mathrm{d}a_4}{\mathrm{d}t} = a_4\left(\lambda_4 + \sum_{j=3}^{4} \lambda_{-jj4} a_j^2\right). \tag{5.1}$$

We obtain the equilibrium solutions for (5.1) by setting the left-hand sides of (5.1) to zero. Evaluating the eigenvalues of the Jacobian matrix about the equilibrium solutions, we obtain the stability conditions for the solutions. For some of these calculations we utilized the computer algebra system REDUCE3. The results are as follows:

(*a*) pure transverse roll $\mathrm{P_S}$

$$a_3^2 = -\lambda_3/\lambda_{-333}, \quad a_4 = 0, \tag{5.2}$$

which is stable if $\lambda_{-333} < 0$ and $\lambda_4 - \lambda_3 \lambda_{-334}/\lambda_{-333} < 0$;

(*b*) pure longitudinal roll $\mathrm{P_L}$

$$a_3 = 0, \quad a_4^2 = -\lambda_4/\lambda_{-444}, \tag{5.3}$$

whose stability condition is given by $\lambda_{-444} < 0$ and $\lambda_3 - \lambda_4 \lambda_{-443}/\lambda_{-444} < 0$;

(*c*) mixed mode M

$$a_3^2 = \frac{\lambda_4 \lambda_{-443} - \lambda_3 \lambda_{-444}}{\det_{34}}, \quad a_4^2 = \frac{\lambda_3 \lambda_{-334} - \lambda_4 \lambda_{-333}}{\det_{34}}, \tag{5.4}$$

which is stable if

$$\mathrm{Re}\,\{a_3^2 \lambda_{-333} + a_4^2 \lambda_{-444} \pm [(a_3^2 \lambda_{-333} + a_4^2 \lambda_{-444})^2 - 4 a_3^2 a_4^2 \det_{34}]^{\frac{1}{2}}\} < 0,$$

where $\det_{jk} \equiv \lambda_{-jjj} \lambda_{-kkk} - \lambda_{-jjk} \lambda_{-kkj}$.

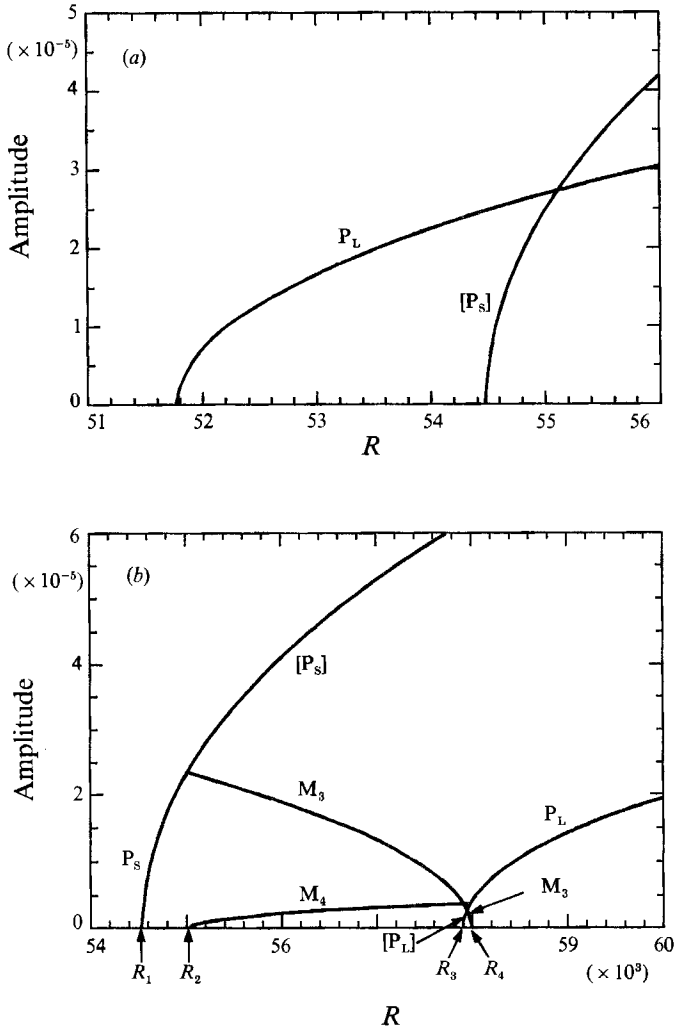

FIGURE 4. Bifurcation diagram for two-mode interaction between transverse stationary rolls and longitudinal rolls. Letters attached to each branch denote the different types of stable equilibrium solution. Letters in a bracket denote unstable equilibrium solutions. $P = 7$; (*a*) $\delta = 1.89°$, (*b*) $\delta = 1.69°$.

Typical bifurcation diagrams are shown in figure 4 for $P = 7$. Linear stability boundaries $\lambda_3 = 0$ and $\lambda_4 = 0$ provide a basis on which to classify the possible equilibrium solutions. Let

$$\delta_{34} = \delta_c^{SL} + 180\left[\frac{\lambda_4^{(P)}\lambda_3^{(G)} - \lambda_4^{(G)}\lambda_3^{(P)}}{\lambda_4^{(G)}\lambda_3^{(\delta)} - \lambda_4^{(\delta)}\lambda_3^{(G)}}\right]\frac{P - P_c}{\pi P P_c}, \tag{5.5}$$

at which λ_3 and λ_4 vanish simultaneously at one value of R. Here (P, δ_c^{SL}) denotes any point on the curve of figure 3 for the S–L interaction. In the neighbourhood of $P = 7$,

$$\delta_{34} \approx -0.021\,15 + 12.716P^{-1}.$$

This is the local expression of the cross-over point between the (S) mode and the (L) mode in figure 3. Moreover, we denote R_1, R_2, R_3, and R_4 as the Rayleigh numbers

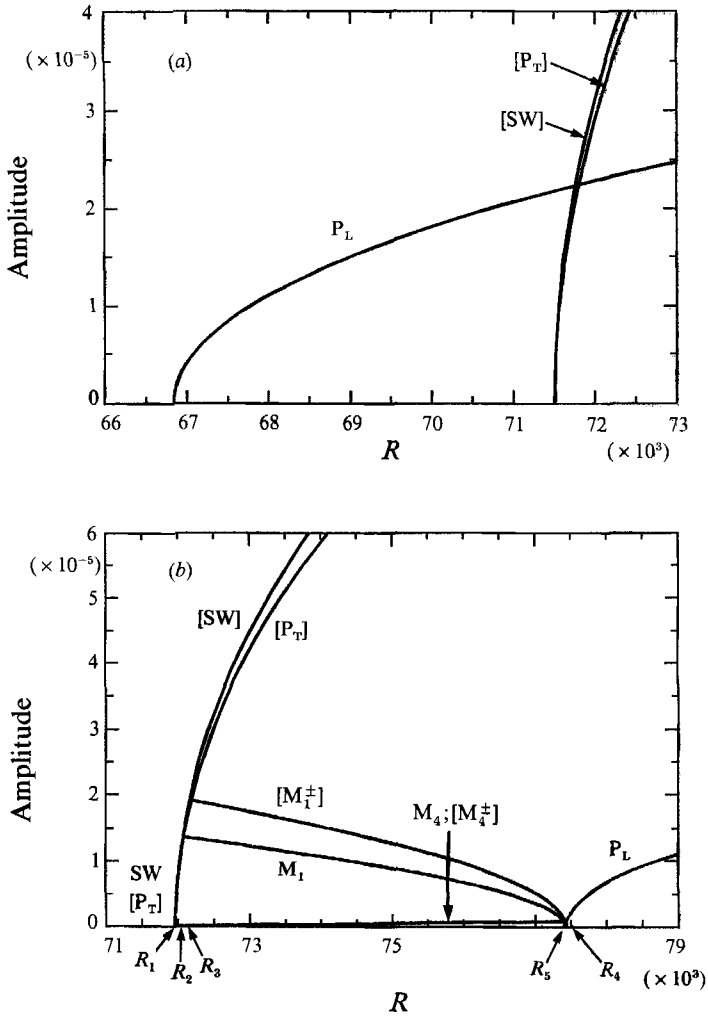

FIGURE 5. Bifurcation diagram for two-mode interaction between transverse travelling waves and longitudinal rolls. $P = 100$; (*a*) $\delta = 1.464°$, (*b*) $\delta = 1.264°$.

at which $A^2_{3P_S} = 0, A^2_{4M} = 0, A^2_{4P_L} = 0$, and $A^2_{3M} = 0$ hold, respeetively; see figure 4. By imposing these conditions in (5.2)–(5.4) and substituting

$$\lambda_j = \epsilon^2[\lambda_j^{(G)} + \tilde{\delta}\lambda_j^{(\delta)} + \tilde{P}\lambda_j^{(P)}]$$
$$= \lambda_j^{(G)}(P_c R_c^{-1} - PR^{-1}) + \lambda_j^{(\delta)}(\delta - \delta_c) + \lambda_j^{(P)}(P_c^{-1} - P^{-1}),$$

we obtain explicit forms of R_n for $n = 1, 2, 3, 4$ which can be summarized as

$$R_n = b_1^{(n)}/(\delta + b_2^{(n)}P^{-1} + b_3^{(n)}). \tag{5.6}$$

We do not list the numerical values of the coefficients $b_1^{(n)}$, $b_2^{(n)}$, and $b_3^{(n)}$, but they are available from the authors.

Now if $\delta > \delta_{34}$, P_L is stable for $R_1 > R \geqslant R_3$, and P_L is stable while P_S is unstable for $R \geqslant R_1$. If $\delta < \delta_{34}$, on the other hand, P_S is stable for $R_1 \leqslant R \leqslant R_2$, M is stable while P_S is unstable for $R_2 \leqslant R \leqslant R_3$, M is stable while P_S and P_L are unstable for $R_3 \leqslant R \leqslant R_4$, and P_L is stable while P_S is unstable for $R \geqslant R_4$. The results are valid for coefficients in table 2. Qualitatively the same bifurcation characteristics are obtained for $P = 0.7$ and we do not show them here.

Before discussing the physical implications of the above bifurcation characteristics, we describe the bifurcation of solutions for the interaction between transverse travelling waves and longitudinal rolls that can occur for $P > P_c^{ST}$. Setting $\epsilon A_j(t) = a_j(t)\,e^{i\theta_j(t)}$ for $j = 1, 2, 4$ yields coupled amplitude equations of the form

$$\left.\begin{aligned} da_1/dt &= a_1(c_1 + c_{111}a_1^2 + c_{221}a_2^2 + c_{441}a_4^2) \equiv a_1 p_1, \\ da_2/dt &= a_2(c_1 + c_{221}a_1^2 + c_{111}a_2^2 + c_{441}a_4^2) \equiv a_2 p_2, \\ da_4/dt &= a_4(c_4 + c_{114}a_1^2 + c_{114}a_2^2 + c_{444}a_4^2) \equiv a_4 p_4, \end{aligned}\right\} \tag{5.7}$$

where $c_j \equiv \mathrm{Re}\,\lambda_j$ for $j = 1, 2, 4$, and $c_{kkj} \equiv \mathrm{Re}\,\lambda_{-kkj}$ for $k = 1, 2, 4$. The possible equilibrium solutions are:

(*a*) travelling wave P_T

$$a_1^2 = -c_1/c_{111}, \quad a_2 = a_4 = 0, \tag{5.8}$$

which is stable if $\partial p_1/\partial a_1^2 < 0$, $p_2 < 0$, and $p_4 < 0$;

(*b*) pure longitudinal roll P_L

$$a_1 = a_2 = 0, \quad a_3^2 = -c_4/c_{444}, \tag{5.9}$$

which is stable if $\partial p_4/\partial a_4^2 < 0$, $p_1 < 0$, and $p_2 < 0$;

(*c*) standing wave SW

$$a_1^2 = a_2^2 = -c_1/(c_{111} + c_{221}), \quad a_4 = 0, \tag{5.10}$$

whose stability condition is given by

$$c_1 > 0, \quad (c_{111} - c_{221})(c_{111} + c_{221}) > 0, \quad p_4 < 0;$$

(*d*) mixed mode $M^{\pm}$

$$a_1^2 = \frac{c_4 c_{441} - c_1 c_{444}}{\det_{14}}, \quad a_2 = 0, \quad a_4^2 = \frac{c_1 c_{114} - c_4 c_{111}}{\det_{14}}, \tag{5.11}$$

whose stability condition is given by $p_2 < 0$ and

$$\mathrm{Re}\,\{c_{111}a_1^2 + c_{444}a_4^2 \pm [(c_{111}a_1^2 + c_{444}a_4^2)^2 - 4a_1^2 a_4^2 \det_{14}]^{\frac{1}{2}}\} < 0;$$

(*e*) mixed mode M

$$\left.\begin{aligned} a_1^2 = a_2^2 &= \frac{(c_1 c_{444} - c_4 c_{441})(c_{221} - c_{111})}{2c_{114}c_{441}(c_{221} - c_{111}) - c_{444}(c_{221}^2 - c_{111}^2)}, \\ a_4^2 &= \frac{-c_4(c_{111}^2 - c_{221}^2) - 2c_1 c_{114}(c_{221} - c_{111})}{2c_{114}c_{441}(c_{221} - c_{111}) - c_{444}(c_{221}^2 - c_{111}^2)}, \end{aligned}\right\} \tag{5.12}$$

which is stable if $\mathrm{Re}\,\lambda < 0$, where λ denotes three roots of the cubic equation

$$\begin{aligned} \lambda^3 - 2(2a_1^2 c_{111} + a_4^2 c_{444})\lambda^2 + 4[a_1^4(c_{111}^2 - c_{221}^2) + 2a_1^2 a_4^2 \det_{14}]\lambda \\ + 8a_1^4 a_4^2[c_{444}(c_{221}^2 - c_{111}^2) + 2c_{114}c_{441}(c_{111} - c_{221})] = 0. \end{aligned}$$

We show typical bifurcation diagrams in figure 5 for $P = 100$. Proceeding as in the S–L interaction case, we let

$$\delta_{14} = \delta_c^{TL} + 180\left[\frac{\lambda_{1r}^{(P)}\lambda_4^{(G)} - \lambda_{1r}^{(G)}\lambda_4^{(P)}}{\lambda_{1r}^{(G)}\lambda_4^{(\delta)} - \lambda_{1r}^{(\delta)}\lambda_4^{(G)}}\right]\frac{P - P_c}{\pi P P_c}, \tag{5.13}$$

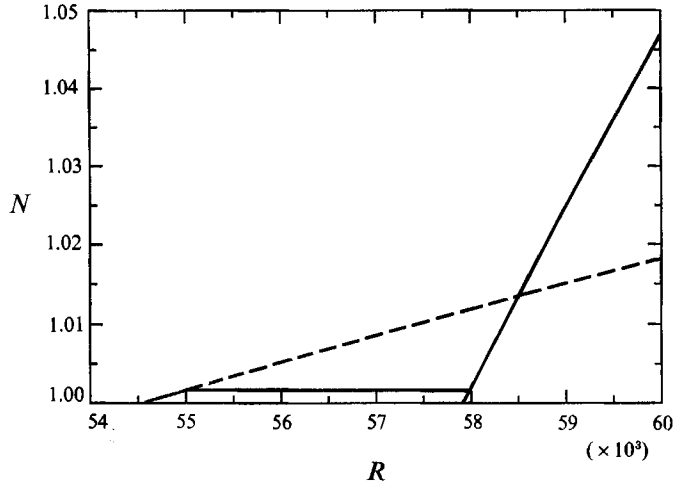

FIGURE 6. Nusselt number for two-mode interaction between transverse stationary rolls and longitudinal rolls for $P = 7$ and $\delta = 1.69°$. Solid line denotes the physically realizable Nusselt number while the dashed line denotes the number associated with unstable pure transverse stationary rolls.

and define R_1, R_2, R_3, R_4, and R_5 such that $A^2_{1P_T} = A^2_{1SW} = 0$, $A^2_{4M} = 0$, $A^2_{4M^\pm} = 0$, $A^2_{1M} = A^2_{1M^\pm} = 0$, and $A^2_{4P_L} = 0$, respectively, where δ_c^{TL} denotes the inclination angle at the cross-over point at the T–L interaction. We write R_n in the form

$$R_n = b_1^{(n)}/(\delta + b_2^{(n)} P^{-1} + b_3^{(n)}). \tag{5.14}$$

The numerical values of the coefficients $b_j^{(n)}$ are available from the authors. In the neighbourhood of the same P, we obtain the local expression for the curve lying between the T and L regions in figure 3 as

$$\delta_{14} \approx 0.7007 + 66.327 P^{-1}.$$

We now classify the possible states. If $\delta > \delta_{14}$, P_L is stable for $R_5 \leqslant R \leqslant R_1$, whereas for $R \geqslant R_1$, P_L is stable while P_T and P_{SW} are unstable. If $\delta < \delta_{14}$, on the other hand, SW is stable while P_T is unstable for $R_1 \leqslant R \leqslant R_2$; M is stable while P_T and SW are unstable for $R_2 \leqslant R \leqslant R_3$; M is stable while P_T, SW, and $M^\pm$ are unstable for $R_3 \leqslant R \leqslant R_5$; M is stable while P_T, SW, $M^\pm$ and P_L are unstable for $R_5 \leqslant R \leqslant R_4$; and P_L is stable while P_T and SW are unstable for $R_4 \leqslant R$. These results are valid for the coefficients given in table 3.

Let us now discuss the physical significance of these bifurcation characteristics. They show that the longitudinal roll is always stable if the critical Rayleigh number for the L mode is less than that for the S and T modes, i.e. $R_c^L \leqslant R_c^S$ and $R_c^L \leqslant R_c^T$. For these cases, therefore, a pure transverse disturbance can never be achieved. On the other hand, if $R_c^L > R_c^S$, a transverse stationary roll appears at first as the pure mode P_S. It thereafter bifurcates into a mixed mode M containing initially both the transverse roll and the longitudinal one, but finally the pure mode P_L becomes the only stable state as the Rayleigh number increases further. The former results agree with those of Richter (1973) for combined Couette–Poiseuille flow while the latter results agree with those of Kropp & Busse (1991*a*) for differentially heated, corotating concentric cylinders. The above is also the case for $R_c^L > R_c^T$. The transverse standing wave SW appears at first. (Note that the travelling wave P_T is always unstable with respect to SW.) It then bifurcates into the mixed mode M

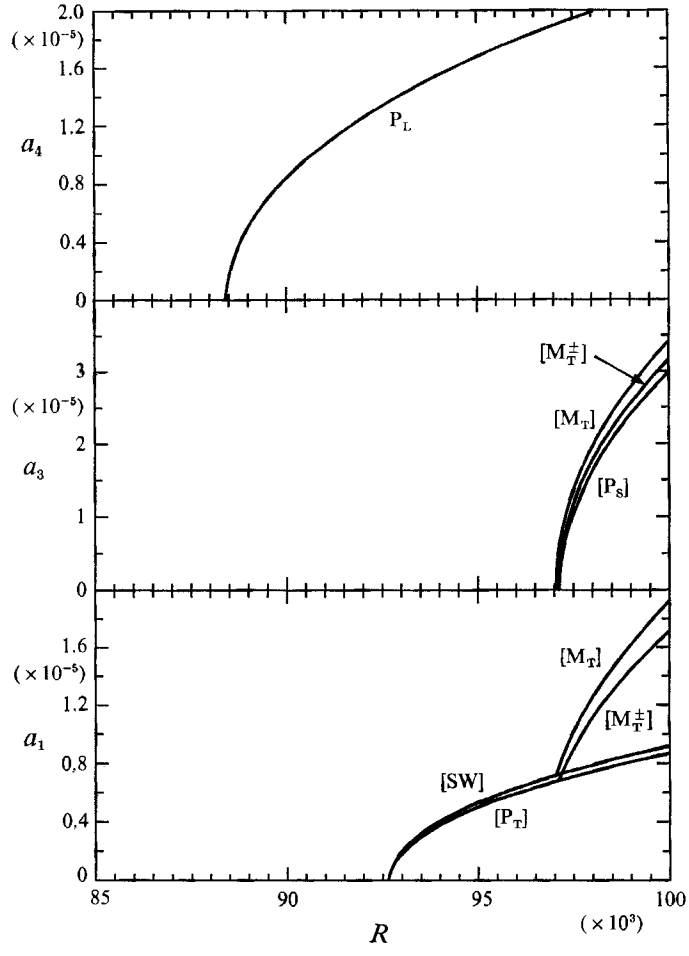

FIGURE 7. Bifurcation diagram for three-mode interaction among transverse stationary rolls, transverse travelling waves, and longitudinal rolls. $P = 12.5$, $\delta = 1.1°$.

composed of the standing wave and the longitudinal roll, but finally the pure mode P_L emerges. Therefore, the longitudinal roll is stable for $\delta \geqslant \delta_c^{SL}$ and $P < P_c$ or $\delta \geqslant \delta_c^{TL}$ and $P > P_c$ at fixed P; transition from the transverse disturbance to the longitudinal roll via a mixed mode occurs otherwise. We now conclude that the longitudinal roll is the disturbance achieved for relatively large values of the Rayleigh number. We have already given more precise criteria for the existence and stability of each of the equilibrium solutions.

In figure 6, we depict the Nusselt number as a function of R at $P = 7$ corresponding to the bifurcation diagram given in figure 4(*b*). The existence of the mixed mode is found to decrease the heat transfer relative to the case of a pure transverse disturbance. The reduction in heat transfer is also obtained for $P = 100$ although we do not show the result here.

We note here that the above analysis does not hold if $R_c^L \gg R_c^S$ or R_c^T (or equivalently, $\delta \ll \delta_c^{SL}$ or $\delta \ll \delta_c^{TL}$ for fixed P, respectively). Instead, a transverse stationary roll or transverse standing wave can be stable, if it exists. Unfortunately, the weakly nonlinear theory consistent to the cubic order cannot determine the range of validity of the present analysis.

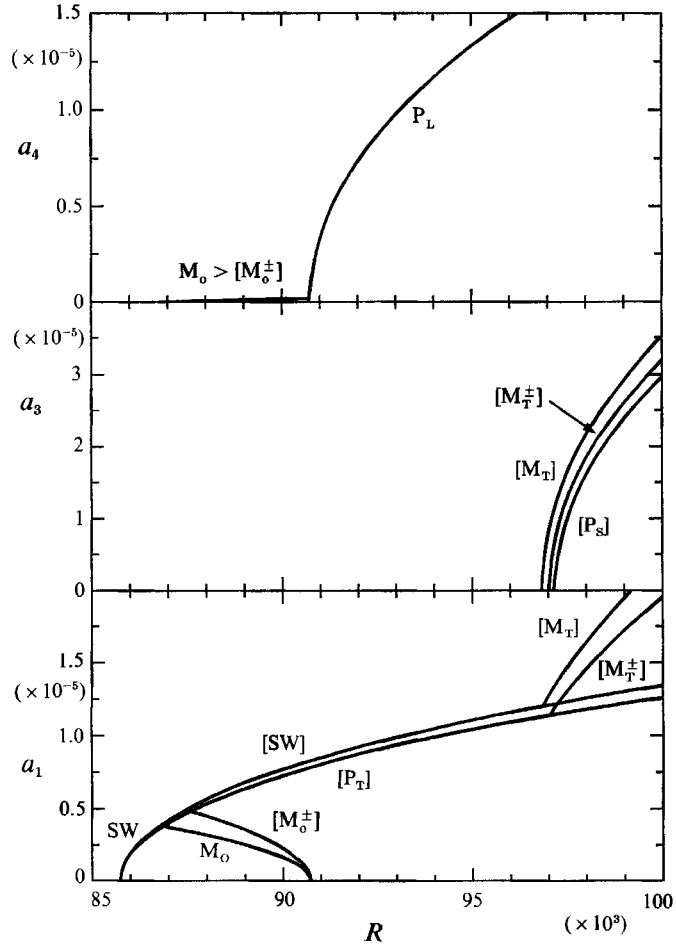

FIGURE 8. As figure 7 but at $P = 12.65$, $\delta = 1.06°$.

For the bifurcation characteristics on the curve of S–T in figure 3 see Fujimura & Mizushima (1991), Kropp & Busse (1991*b*), or Fujimura (1992). For brevity we do not describe these bifurcation characteristics again in the present paper.

6. Bifurcation for three-mode interaction

In the neighbourhood of the cross-over region among three modes, S, T, and L, the above characteristics partly hold, but some new equilibrium solutions appear which will now be described in detail. Let $\epsilon A_j(t) = a_j(t)\,e^{i\theta_j(t)}$. Then the coupled amplitude equations for three-mode interaction between S, T and L are

$$\left.\begin{aligned} da_1/dt &= a_1(c_1 + c_{111}a_1^2 + c_{221}a_2^2 + c_{331}a_3^2 + c_{441}a_4^2) \equiv a_1 p_1, \\ da_2/dt &= a_2(c_1 + c_{221}a_1^2 + c_{111}a_2^2 + c_{331}a_3^2 + c_{441}a_4^2) \equiv a_2 p_2, \\ da_3/dt &= a_3(c_3 + c_{113}a_1^2 + c_{113}a_2^2 + c_{333}a_3^2 + c_{443}a_4^2) \equiv a_3 p_3, \\ da_4/dt &= a_4(c_4 + c_{114}a_1^2 + c_{114}a_2^2 + c_{334}a_3^2 + c_{444}a_4^2) \equiv a_4 p_4, \end{aligned}\right\} \tag{6.1}$$

where $c_j \equiv \mathrm{Re}\,\lambda_j$ for $j = 1, 2, 3, 4$, and $c_{kkj} \equiv \mathrm{Re}\,\lambda_{-kkj}$ for $k = 1, 2, 3, 4$.

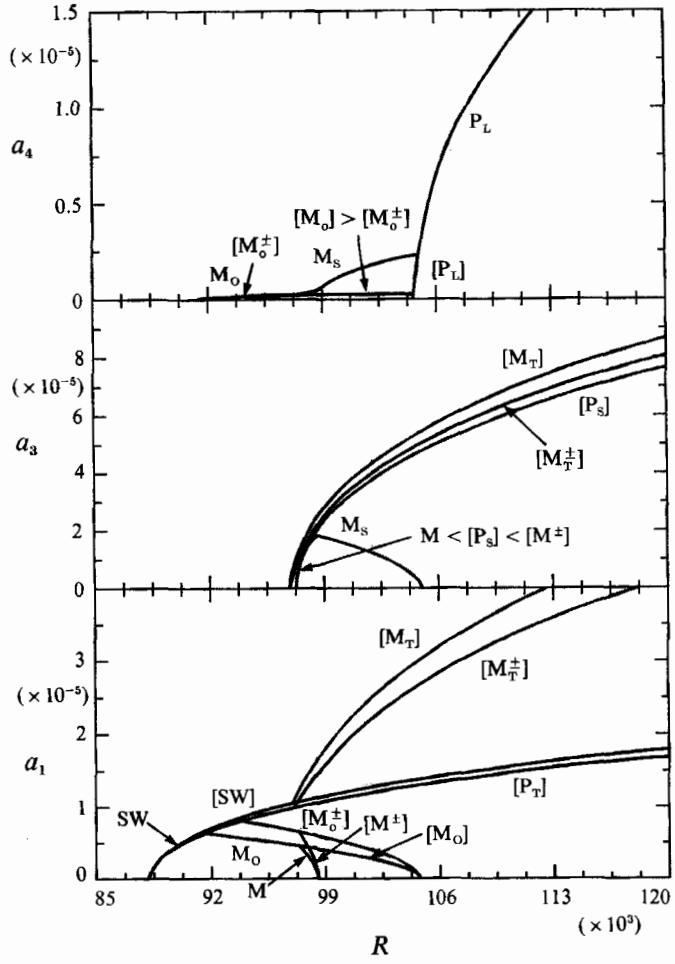

FIGURE 9. As figure 7 but at $P = 12.6$, $\delta = 0.92°$.

The coupled amplitude equations possess 11 different equilibrium solutions. They are:

(i) pure mode P_T: $a_1^2 \neq 0$, $a_2^2 = a_3^2 = a_4^2 = 0$;
(ii) standing wave SW: $a_1^2 = a_2^2 \neq 0$, $a_3^2 = a_4^2 = 0$;
(iii) pure more P_S: $a_1^2 = a_2^2 = a_4^2 = 0$, $a_3^2 \neq 0$;
(iv) pure mode P_L: $a_1^2 = a_2^2 = a_3^2 = 0$, $a_4^2 \neq 0$;
(v) transverse mixed mode M_T: $a_1^2 = a_2^2 \neq 0$, $a_3^2 \neq 0$, and $a_4^2 = 0$;
(vi) mixed mode M_O: $a_1^2 = a_2^2 \neq 0$, $a_3^2 = 0$, and $a_4^2 \neq 0$;
(vii) transverse mixed mode $M_T^{\pm}$: $a_1^2 \neq 0$, $a_2^2 = a_4^2 = 0$, and $a_3^2 \neq 0$;
(viii) mixed mode $M_O^{\pm}$: $a_1^2 \neq 0$, $a_2^2 = a_3^2 = 0$, and $a_4^2 \neq 0$;
(ix) mixed mode M: $a_1^2 = a_2^2 \neq 0$, $a_3^2 \neq 0$, and $a_4^2 \neq 0$;
(x) mixed mode M_S: $a_1^2 = a_2^2 = 0$, $a_3^2 \neq 0$, and $a_4^2 \neq 0$;
(xi) mixed mode $M^{\pm}$: $a_1^2 \neq 0$, $a_2^2 = 0$, $a_3^2 \neq 0$, and $a_4^2 \neq 0$.

We list the explicit forms of the above solutions and their stability conditions in the Appendix. The bifurcation characteristics have a richer variety in than the cases of §5. We demonstrate typical examples of the bifurcation diagrams in figures 7–12. Although they are much more complicated than the diagrams for the two-mode

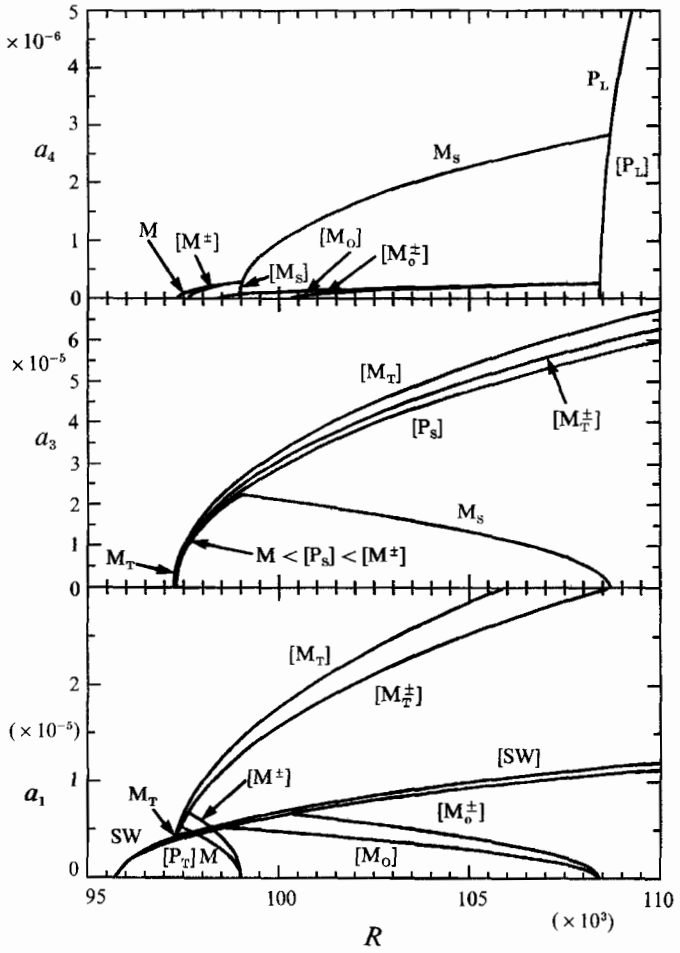

FIGURE 10. As figure 7 but at $P = 12.45$, $\delta = 0.9°$.

interactions, each branch of the diagram is qualitatively consistent with the ones in figures 4 and 5, and with figures 1 and 2 of Fujimura (1992) except for mixed modes M and $M^{\pm}$.

Besides the δ_{34} and δ_{14} defined in §5, we introduce

$$\delta_{13} = \delta_c^{ST} + 180\left[\frac{\lambda_{1r}^{(P)}\lambda_3^{(G)} - \lambda_{1r}^{(G)}\lambda_3^{(P)}}{\lambda_{1r}^{(G)}\lambda_3^{(\delta)} - \lambda_{1r}^{(\delta)}\lambda_3^{(G)}}\right]\frac{P - P_c}{\pi P P_c}. \tag{6.2}$$

In the neighbourhood of the cross-over region among the three modes, S, T, and L, the local expressions for the curves in figure 3 are

$$\delta_{13} \approx -387.28 + 4822.5P^{-1}, \quad \delta_{14} \approx 7.5066 - 80.731P^{-1},$$
$$\delta_{34} \approx -0.0067762 + 12.585P^{-1}.$$

We also define R_{jk} for $j = 1, 2, 3, 4$ and $1 \leqslant k \leqslant 11$ such that $A_j^{(k)2} = 0$ at $R = R_{jk}$. Here k denotes the label of each equilibrium solution according to the above classification. The R_{jk} are given in the form

$$R_{jk} = b_1^{(j,k)}/(\delta + b_2^{(j,k)}P^{-1} + b_3^{(j,k)}). \tag{6.3}$$

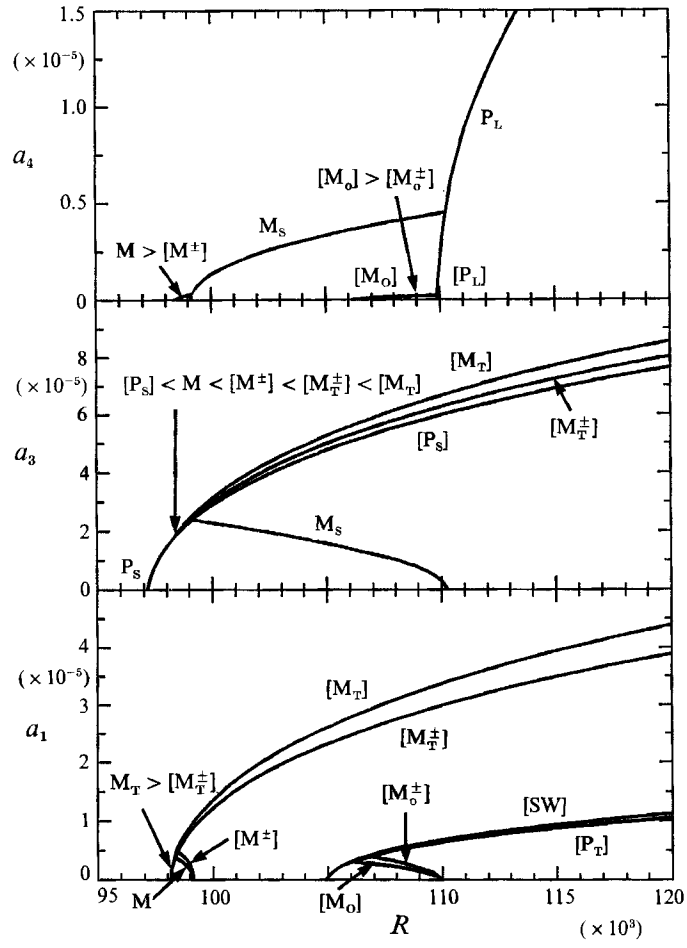

FIGURE 11. As figure 7 but at $P = 12.3$, $\delta = 0.9°$.

The numerical values of $b_m^{(j,k)}$ evaluated at the cross-over point are available from the authors.

The classification of the stable equilibrium solutions is tabulated in table 5. Here $\delta_{35,46}$ is the δ at which $A^2_{3M_T}$ and $A^2_{4M_O}$ vanish simultaneously, and $\delta_{15,410}$ is the δ at which $A^2_{3M_T}$ and $A^2_{4M_S}$ vanish simultaneously. In the neighbourhood of the cross-over region, they are

$$\delta_{35,46} \approx 315.13P^{-1} - 24.366, \quad \delta_{15,410} \approx -60.7603P^{-1} + 5.89868.$$

From the above discussions, we conclude that only the longitudinal roll, P_L, is achieved in the sector where $\delta > \delta_{34}$ and $\delta > \delta_{14}$. Outside this sector, another equilibrium solution exists stably for relatively low Rayleigh numbers. But eventually the pure longitudinal roll dominates for high Rayleigh numbers.

7. Discussion and conclusions

We derived the coupled amplitude equations for two-mode interactions between S and L and between T and L, and three-mode interactions among S, T, and L on a weakly nonlinear basis for thermal convection in an inclined slot of infinite extent.

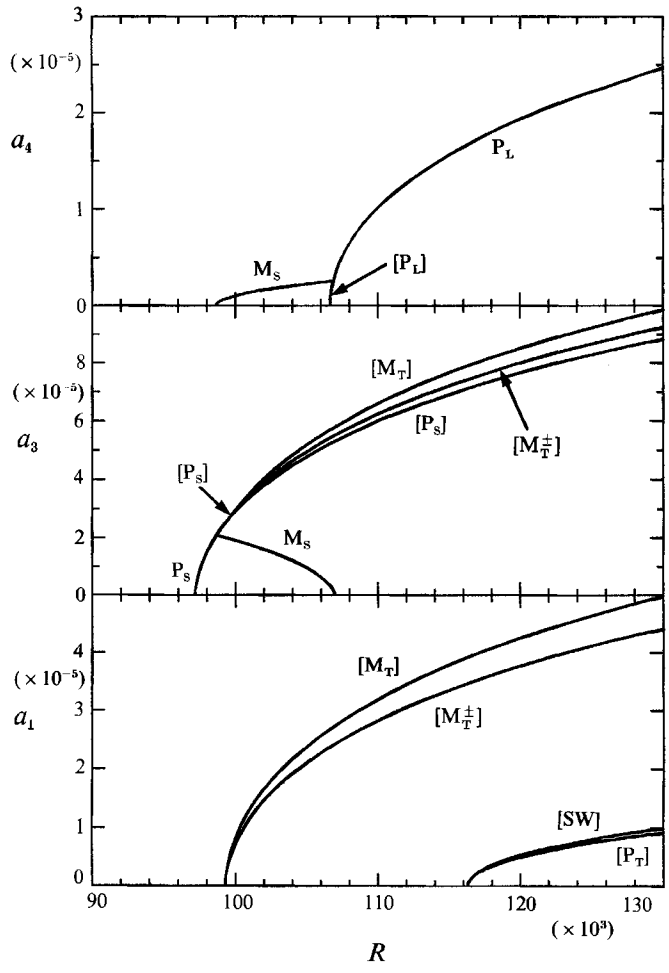

FIGURE 12. As figure 7 but at $P = 12.15$, $\delta = 0.94°$.

We found that pure longitudinal rolls dominate the dynamics for some range of the parameter set in the (P, δ)-plane while stable transverse disturbances (P_S or SW) bifurcate first into a stable mixed mode and thereafter to stable longitudinal rolls which exist in the remaining part of the (P, δ)-plane. In the neighbourhood of the cross-over region for the three-mode interaction, the bifurcation characteristics have a rich variety. Possible stable solutions correspond to a pure transverse stationary roll P_S, a standing wave SW, mixed modes M, M_S, M_T, and M_O, and a pure longitudinal roll P_L. Any mode composed of a travelling wave propagating in one direction is concluded to be unstable. Cubic-order analysis given in the present paper is considered to be valid within 10% error judging from figure 5 of Fujimura & Mizushima (1991) in which the validity of the cubic-order analysis is discussed in comparison with fully numerical results for the equilibrium solutions.

It should be remembered that the present results hold only when both of the two modes or all of the three modes become critical for nearly the same value of the control parameter. Also when $R \gg R_c^L$, the longitudinal rolls can develop a wavy instability which introduces three-dimensionality into the flow; see Clever & Busse (1977) and Busse & Clever (1992). However, this secondary instability is unrelated to the transverse disturbance discussed here (e.g. the wavy instability has an infinite

$\delta > \delta_{34}$, $\delta > \delta_{14}$	P_L	for	$R > R_{44}$
$\delta > \delta_{34}$, $\delta < \delta_{14}$	SW	for	$R_{11} = R_{12} \leqslant R \leqslant R_{46}$
	M_O	for	$R_{46} \leqslant R \leqslant R_{44}$
	P_L	for	$R_{44} \leqslant R$
$\delta < \delta_{34}$, $\delta > \delta_{35,46}$	SW	for	$R_{11} = R_{12} \leqslant R \leqslant R_{46}$
	M_O	for	$R_{46} \leqslant R \leqslant R_{39}$
	M	for	$R_{39} \leqslant R \leqslant R_{19} = R_{111}$
	M_S	for	$R_{19} = R_{111} \leqslant R \leqslant R_{310}$
	P_L	for	$R_{310} \leqslant R$
$\delta < \delta_{35,46}$, $\delta > \delta_{13}$	SW	for	$R_{11} = R_{12} \leqslant R \leqslant R_{35}$
	M_T	for	$R_{35} \leqslant R \leqslant R_{39}$
	M	for	$R_{39} \leqslant R \leqslant R_{19} = R_{111}$
	M_S	for	$R_{19} = R_{111} \leqslant R \leqslant R_{310}$
	P_L	for	$R_{310} \leqslant R$
$\delta < \delta_{13}$, $\delta < \delta_{15,410}$	P_S	for	$R_{33} \leqslant R \leqslant R_{15} = R_{17}$
	M_T	for	$R_{15} = R_{17} \leqslant R \leqslant R_{49}$
	M	for	$R_{49} \leqslant R \leqslant R_{19} = R_{111}$
	M_S	for	$R_{19} = R_{111} \leqslant R \leqslant R_{310}$
	P_L	for	$R_{310} \leqslant R$
$\delta > \delta_{15,410}$, $\delta < \delta_{34}$	P_S	for	$R_{33} \leqslant R \leqslant R_{410}$
	M_S	for	$R_{410} \leqslant R \leqslant R_{310}$
	P_L	for	$R_{310} \leqslant R$

TABLE 5. Classification of the stable equilibrium solutions for the three-mode interaction in the neighbourhood of $(P, R, \delta) = (12.420013, 97216.060, 1.0065474)$.

critical wavelength), and there is no reason to think that the linear transverse modes are important when $R_c^L \ll R_c^T$ or R_c^S even if $R > R_c^T$ or R_c^S. The situation when $R_c^T \ll R_c^L$ or $R_c^S \ll R_c^L$ is possibly quite different. For instance, figure 4(*b*) indicates that three-dimensionality via a mixed mode sets in when $R < R_c^L$, i.e. the component of the mixed mode corresponding to the longitudinal rolls sets in *subcritically*. It is therefore conceivable that the mixed mode state can exist even if $R_c^S \ll R_c^L$, although a separate analysis is required to determine whether this can actually occur. Such an analysis would require calculation of the transverse mode for values of Rayleigh number well above critical and would have to consider secondary instability of the transverse mode to disturbances of a type more general than only of the longitudinal roll form.

We depict stability diagrams in the (R, δ)-plane for $P = 7$ in figure 13. Because of the constraints of the cubic-order analysis, we cannot reduce the inclination angle to 0°. Our conjecture based on the diagrams for small values of δ is that $R_3 \to \infty$ as $\delta \to 0$ whereas the curve for R_2 goes to the left for a while, becoming steeper, and eventually becoming vertical, and thereafter bends back to the right. Curves R_2 and R_4 are considered to merge at some small value of δ. Of course, R_1 remains finite for $\delta \to 0$.

It is of interest to compare the present results to those of Brand *et al.* (1991) for the case of heated channel flow; cf. their figure 1 showing results in the (R, Re)-plane. For their case, transverse rolls are critical for low values of Re and longitudinal rolls are critical for large values of Re. One might be tempted to simply substitute δ for Re in order to make a comparison but it should be realized that the two cases are most similar when $\delta \approx 90°$, not $\delta \approx 0°$. For instance, in their case, both modes exist on a linear basis as $Re \to 0$ and, for $Re > 0$, the values of R_c for both modes can

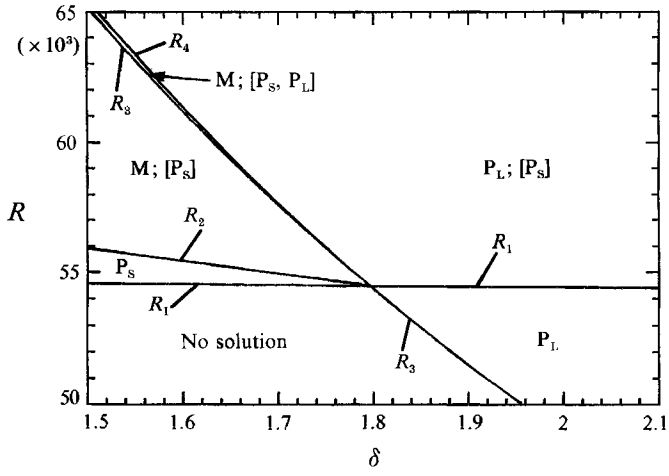

FIGURE 13. Stability diagram for two-mode interaction between transverse stationary rolls and longitudinal rolls at $P = 7$ and $\delta = 1.69°$. R_1, R_2, R_3, and R_4 correspond to R_n in (5.6).

coincide for a suitable choice of the aspect ratio. In the present case, longitudinal rolls simply do not exist as $\delta \to 0$ and, furthermore, it is impossible to have both longitudinal and transverse disturbances occurring simultaneously if $P \leqslant 0.263\,897$ (for $\delta \neq 90°$). It should also be understood that Brand *et al.* (1991) used model amplitude equations with 'typical' values chosen for the interaction coefficients, whereas the present work uses an asymptotic method valid for sufficiently small supercritical values of R and determines the interaction coefficients on the basis of the governing equations. Finally, Brand *et al.* consider a problem with boundary conditions imposed over a finite interval in the flow direction whereas we consider the horizontally unbounded case. With these caveats, the following comparison is made. For a fixed supercritical value of the Rayleigh number, pure transverse rolls exist for low values of Re and pure longitudinal rolls exist at high values of Re. Most of the numerical results of Brand *et al.* (1991) are given for a fixed value of Re as R increases, which is the manner of presentation used in this paper. In most of their results, the Reynolds number is taken to be equal to two, whereas the cross-over value on the basis of linear analysis is 1.5. For $Re = 2$, only longitudinal rolls were found for R up to about $1.23R_c$. Thereafter, transverse rolls appear and begin to displace longitudinal rolls, starting from the downstream end. Over most of the length L, either longitudinal or transverse modes exist. Although a different form of mixed convection than discussed here, this pattern implies that both modes can exist at the same values of Re and R. Our results do not indicate that such a mixed state is possible, starting from longitudinal rolls, as R increases. At a Reynolds number of 1.5 and $R = 1.2R_c$, only transverse rolls exist but, unfortunately, no information is given at values of R closer to critical. No information is given for $Re < 1.5$ when transverse modes become unstable first. Hence, there does not seem to be enough information available in the cross-over regime to perform a meaningful comparison. For slightly different values for the interaction coefficients, Brand *et al.* (1991) found that a mixed mode state of the type described in this paper is possible for $R = 1.165R_c$ and $Re = 2$, which is reassuring. The result indicates that more accurate calculation of the numerical coefficients for the channel flow case is highly desirable.

Finally, we note that the bifurcation characteristics obtained by Kropp & Busse (1991*a*) in corotating concentric cylinders with different temperatures agree with the

ones in figure 4(*b*) of the present paper, at least qualitatively. Because their results are also based on the actual numerical coefficients of the amplitude equations consistent with the governing equations, the bifurcation characteristics obtained in the present paper and by Kropp & Busse would seem to be the appropriate ones for bifurcations involving a transition via a mixed mode.

R.E.K. would like to thank the administrative staff of the Japan Atomic Energy Research Institute for arranging his visit to JAERI during the Fall of 1991 while on sabbatical leave from UCLA.

Appendix. Equilibrium solutions for three-mode interaction and their stability conditions

(i) pure mode $\mathrm{P_T}$

$$a_1^2 = -c_1/c_{111}, \quad a_2 = a_3 = a_4 = 0,$$

which is stable if $\partial p_1/\partial a_1^2 < 0$, $p_2 < 0$, $p_3 < 0$, and $p_4 < 0$;

(ii) standing wave SW

$$a_1^2 = a_2^2 = -c_1/(c_{111}+c_{221}), \quad a_3 = a_4 = 0,$$

whose stability condition is given by $c_1 > 0$, $(c_{111}-c_{221})(c_{111}+c_{221}) > 0$, $p_3 < 0$, and $p_4 < 0$;

(iii) pure mode $\mathrm{P_S}$

$$a_1 = a_2 = a_4 = 0, \quad a_3^2 = -c_3/c_{333},$$

which is stable if $\partial p_3/\partial a_3^2 < 0$, $p_1 < 0$, $p_2 < 0$, and $p_4 < 0$;

(iv) pure mode $\mathrm{P_L}$

$$a_1 = a_2 = a_3 = 0, \quad a_4^2 = -c_4/c_{444},$$

whose stability condition is given by $\partial p_4/\partial a_4^2 < 0$, $p_1 < 0$, $p_2 < 0$, and $p_3 < 0$;

(v) transverse mixed mode $\mathrm{M_T}$

$$a_1^2 = a_2^2 = \frac{(c_1 c_{333} - c_3 c_{331})(c_{221} - c_{111})}{2c_{113} c_{331}(c_{221} - c_{111}) - c_{333}(c_{221}^2 - c_{111}^2)},$$

$$a_3^2 = \frac{-c_3(c_{111}^2 - c_{221}^2) - 2c_1 c_{113}(c_{221} - c_{111})}{2c_{113} c_{331}(c_{221} - c_{111}) - c_{333}(c_{221}^2 - c_{111}^2)}, \quad a_4 = 0,$$

which is stable if $p_4 < 0$ and $\mathrm{Re}\,\lambda < 0$, where λ denotes three roots of the cubic equation

$$\lambda^3 - 2(2a_1^2 c_{111} + a_3^2 c_{333})\lambda^2 + 4[a_1^4(c_{111}^2 - c_{221}^2) + 2a_1^2 a_3^2 \det_{13}]\,\lambda + 8a_1^4 a_3^2[c_{333}(c_{221}^2 - c_{111}^2) + 2c_{113} c_{331}(c_{111} - c_{221})] = 0;$$

(vi) mixed mode $\mathrm{M_O}$

$$a_1^2 = a_2^2 = \frac{(c_1 c_{444} - c_4 c_{441})(c_{221} - c_{111})}{2c_{114} c_{441}(c_{221} - c_{111}) - c_{444}(c_{221}^2 - c_{111}^2)},$$

$$a_3 = 0, \quad a_4^2 = \frac{-c_4(c_{111}^2 - c_{221}^2) - 2c_1 c_{114}(c_{221} - c_{111})}{2c_{114} c_{441}(c_{221} - c_{111}) - c_{444}(c_{221}^2 - c_{111}^2)},$$

which is stable if $p_3 < 0$ and $\mathrm{Re}\,\lambda < 0$, where λ denotes three roots of the cubic equation

$$\lambda^3 - 2(2a_1^2 c_{111} + a_4^2 c_{444})\lambda^2 + 4[a_1^4(c_{111}^2 - c_{221}^2) + 2a_1^2 a_4^2 \det_{14}]\lambda + 8a_1^4 a_4^2[c_{444}(c_{221}^2 - c_{111}^2) + 2c_{114}c_{441}(c_{111} - c_{221})] = 0;$$

(vii) transverse mixed mode $\mathrm{M}_{\mathrm{T}}^{\pm}$

$$a_1^2 = \frac{c_3 c_{331} - c_1 c_{333}}{\det_{13}}, \quad a_2 = a_4 = 0, \quad a_3^2 = \frac{c_1 c_{13} - c_3 c_{111}}{\det_{13}},$$

whose stability condition is given by $p_2 < 0$, $p_4 < 0$, and

$$\mathrm{Re}\,\{c_{111}a_1^2 + c_{333}a_3^2 \pm [(c_{111}a_1^2 + c_{333}a_3^2)^2 - 4a_1^2 a_3^2 \det_{13}]^{\frac{1}{2}}\} < 0;$$

(viii) mixed mode $\mathrm{M}_{\mathrm{O}}^{\pm}$

$$a_1^2 = \frac{c_4 c_{441} - c_1 c_{444}}{\det_{14}}, \quad a_2 = a_3 = 0, \quad a_4^2 = \frac{c_1 c_{114} - c_4 c_{111}}{\det_{14}}.$$

The solution is stable if $p_2 < 0$, $p_3 < 0$, and

$$\mathrm{Re}\,\{c_{111}a_1^2 + c_{444}a_4^2 \pm [(c_{111}a_1^2 + c_{444}a_4^2)^2 - 4a_1^2 a_4^2 \det_{14}]^{\frac{1}{2}}\} < 0;$$

(ix) mixed mode M

$$a_1^2 = f/q, \quad a_2 = a_1, \quad a_3^2 = g/q, \quad a_4^2 = h/q,$$

where

$$f = -(c_1 \det_{34} - c_{444}c_{331}c_3 + c_{334}c_{441}c_3 + c_{443}c_{331}c_4 - c_{333}c_{441}c_4)(c_{221} - c_{111}),$$

$$g = (c_{443}c_4 - c_{444}c_3)(c_{221}^2 - c_{111}^2) + 2(c_{444}c_{113}c_1 - c_{114}c_{443}c_1 + c_{114}c_{441}c_3 - c_{113}c_{441}c_4)(c_{221} - c_{111}),$$

$$h = -(c_{333}c_4 - c_{334}c_3)(c_{221}^2 - c_{111}^2) - 2(c_{334}c_{113}c_1 - c_{113}c_{331}c_4 - c_{114}c_{333}c_1 + c_{114}c_{331}c_3)(c_{221} - c_{111}),$$

$$q = (c_{444}c_{333} - c_{334}c_{443})(c_{221}^2 - c_{111}^2) + 2(c_{334}c_{113}c_{441} - c_{444}c_{113}c_{331} + c_{114}c_{443}c_{331} - c_{114}c_{333}c_{441})(c_{221} - c_{111}).$$

Stability condition is given by $\mathrm{Re}\,\lambda < 0$ where λ denotes four roots of the quartic equation

$$\begin{aligned}
&-\lambda^4 + 2(2a_1^2 c_{111} + a_3^2 c_{333} + a_4^2 c_{444})\lambda^3 \\
&+ 4[a_1^4(c_{221}^2 - c_{111}^2) - 2a_1^2 a_3^2 \det_{13} - 2a_1^2 a_4^2 \det_{14} - a_3^2 a_4^2 \det_{34}]\lambda^2 \\
&+ 8a_1^2[-a_1^2(a_3^2 c_{333} + a_4^2 c_{444})(c_{221}^2 - c_{111}^2) + 2a_1^2(a_3^2 c_{113}c_{331} + a_4^2 c_{114}c_{441})(c_{221} - c_{111}) \\
&\quad + 2a_3^2 a_4^2 c_{444}(c_{333}c_{111} - c_{113}c_{331}) - 2a_3^2 a_4^2 c_{334}(c_{443}c_{111} - c_{113}c_{441}) \\
&\quad + 2a_3^2 a_4^2 c_{114}(c_{443}c_{331} - c_{333}c_{441})]\lambda \\
&+ 16a_1^4 a_3^2 a_4^2[\det_{34}(c_{221}^2 - c_{111}^2) \\
&\quad + 2(c_{334}c_{113}c_{441} - c_{444}c_{113}c_{331} + c_{114}c_{443}c_{331} - c_{114}c_{333}c_{441})(c_{221} - c_{111})] = 0;
\end{aligned}$$

(x) mixed mode M_{S}

$$a_1 = a_2 = 0, \quad a_3^2 = \frac{c_4 c_{443} - c_3 c_{444}}{\det_{34}}, \quad a_4^2 = \frac{c_3 c_{334} - c_4 c_{333}}{\det_{34}},$$

which is stable if $p_1 < 0$ $p_2 < 0$ and

$$\mathrm{Re}\,\{c_{333}a_3^2 + c_{444}a_4^2 \pm [(c_{333}a_3^2 + c_{444}a_4^2)^2 - 4a_3^2 a_4^2 \det_{34}]^{\frac{1}{2}}\} < 0;$$

(xi) mixed mode $\mathrm{M}^{\pm}$

$$a_1^2 = f/q, \quad a_2 = 0, \quad a_3^2 = g/q, \quad a_4^2 = h/q,$$

where

$$f = -[c_{333}(c_{444}c_1 - c_{441}c_4) + c_{331}(c_{443}c_4 - c_{444}c_3) + c_{334}(c_{441}c_3 - c_{443}c_1)],$$
$$g = c_{113}(c_{444}c_1 - c_{441}c_4) + c_{111}(c_{443}c_4 - c_{444}c_3) + c_{114}(c_{441}c_3 - c_{443}c_1),$$
$$h = -[c_{333}(c_{111}c_4 - c_{114}c_1) + c_{331}(c_{114}c_3 - c_{113}c_4) + c_{334}(c_{113}c_1 - c_{111}c_3)],$$
$$q = c_{333}(c_{111}c_{444} - c_{114}c_{441}) + c_{113}(c_{441}c_{334} - c_{331}c_{444}) + c_{443}(c_{331}c_{114} - c_{111}c_{334}).$$

Stability condition is given by $\mathrm{Re}\,\lambda < 0$ and $p_2 < 0$, where λ denotes three roots of the cubic equation

$$\lambda^3 - 2(c_{111}a_1^2 + c_{333}a_3^2 + c_{444}a_4^2)\lambda^2 + 4[a_1^2 a_3^2 \det_{13} + a_1^2 a_4^2 \det_{14} + a_3^2 a_4^2 \det_{34}]\lambda$$
$$+ 8a_1^2 a_3^2 a_4^2[c_{444}(c_{113}c_{331} - c_{333}c_{111}) + c_{334}(c_{443}c_{111} - c_{113}c_{441}) + c_{114}(c_{333}c_{441} - c_{443}c_{331})] = 0.$$

REFERENCES

Bergholz, R. F. 1978 *J. Fluid Mech.* **84**, 743–768.

Brand, H. R., Deissler, R. J. & Ahlers, G. 1991 *Phys. Rev.* A **43**, 4262–4268.

Busse, F. H. & Clever, R. M. 1992 *J. Engng Maths* **26**, 1–20.

Chen, M. M. & Whitehead, J. A. 1968 *J. Fluid Mech.* **31**, 1–15.

Chen, Y.-M. & Pearlstein, A. J. 1989 *J. Fluid Mech.* **198**, 513–541.

Clever, R. M. & Busse, F. H. 1977 *J. Fluid Mech.* **81**, 107–127.

Fujimura, K. 1992 *Eur. J. Mech.* B/*Fluids* **11**, 461–464.

Fujimura, K. & Mizushima, J. 1991 *Eur. J. Mech.* B/*Fluids* **10**, Suppl. No. 2, 25–30.

Gershuni, G. Z. & Zhukhovitskii, E. M. 1969 *Prikl. Mat. Mekh.* **33**, 855–860.

Hart, J. E. 1971 *J. Fluid Mech.* **47**, 547–576.

Hollands, K. G. T. & Konicek, L. 1973 *Intl J. Heat Mass Transfer* **16**, 1467–1476.

Kirchartz, K. R. & Oertel, H. 1988 *J. Fluid Mech.* **192**, 249–286.

Korpela, S. A. 1974 *Intl J. Heat Mass Transfer* **17**, 215–222.

Kropp, M. & Busse, F. H. 1991*a* *Phys. Fluids* A **3**, 2988–2994.

Kropp, M. & Busse, F. H. 1991*b* In *Bifurcation and Chaos* (ed. T. Küpper, R. Seydel & F. W. Schneider), pp. 217–223. Birkhäuser.

Luijkx, L. M., Platten, J. K. & Legros, J. C. 1981 *Intl J. Heat Mass Transfer* **24**, 1287–1292.

Müller, H. W., Lücke, M. & Kamps, M. 1989 *Europhys. Lett.* **10**, 451–456.

Müller, H. W., Lücke, M. & Kamps, M. 1992 *Phys. Rev.* A **45**, 3714–3726.

Ouazzani, M. T., Platten, J. K. & Mojtabi, A. 1990 *Intl J. Heat Mass Transfer* **33**, 1417–1427.

Platten, J. K. & Legros, J. C. 1984 *Convection in Liquids*. Springer.

Richter, F. M. 1973 *J. Geophys. Res.* **78**, 8735–8745.

Richter, F. M. & Parsons, B. 1975 *J. Geophys. Res.* **80**, 2529–2541.

Rosenblat, S. 1982 *J. Fluid Mech.* **122**, 395–410.

Shadid, J. N. & Goldstein, R. J. 1990 *J. Fluid Mech.* **215**, 61–84.